Int. J. Electrochem. Sci., 11 **(2016)** 2579 - 2594

International Journal of
ELECTROCHEMICAL
SCIENCE
www.electrochemsci.org

Immobilized Ammoniated Ruthenium Oxychloride on Functionalized Carbon Nanotubes as a Modifier for Simultaneous Determination of Biocompounds

Farideh Hosseini-Narouei[1], *Meissam Noroozifar*[1,*], *Mozhgan Khorasani-Motlagh*[2]

[1]Analytical Research Laboratory, Department of Chemistry, University of Sistan and Baluchestan, Zahedan, P.O. Box 98167-674, Iran
[2]Inorganic Research Laboratory, Department of Chemistry, University of Sistan and Baluchestan, Zahedan, Iran
[*]E-mail: mnoroozifar@chem.usb.ac.ir

Received: 07 November 2015 / *Accepted:* 25 January 2016 / *Published:* 1 March 2016

Modified glassy carbon electrode with immobilized ammoniated ruthenium oxychloride on multi-walled carbon nanotube has been used for the simultaneous determination of ascorbic acid (AA), dopamine (DA), uric acid (UA) and tryptophan (Trp). The modified electrode can well separate quaternary mixture containing AA, DA, UA and Trp from each other at 0.09, 0.323, 0.511 and 0.728 V. The measurements were performed using cyclic and liner sweeping voltammetry in a phosphate buffer solution in pH 4.0. Under optimum conditions, this modified electrode showed a linear response up to 176.8, 300.0, 310.0 and 326.0 µM with detection limits 1.5, 0.64, 0.57 and 0.61 µM for AA, DA, UA and Trp, respectively. The analytical performance of the modified electrode has been evaluated in human serum and urine samples.

Keywords: Ammoniated ruthenium oxychloride**,** multi-walled carbon nanotube, simultaneous determination, serum, urine**.**

1. INTRODUCTION

Ascorbic acid (AA) as an important vitamin (called Vitamin C) is present in fruits and vegetables. This compound is added as an antioxidant for stabilization of color and aroma to foodstuffs in commercial products [1]. In other hand, AA plays a significant role in clinical diagnostics and neurochemistry applications. It is essential compound for the prevention and treatment of common cold and cancer [2]. Dopamine (DA) plays a critical role neurochemistry systems [3]. It is significant to determine the DA level in diagnose Parkinson's disease and neurotransmission processes. Uric acid

(UA) is an important compound in clinical samples for indicating several diseases, such as hyperuricaemia, gout, and Lesch-Nyhan syndrome [4]. The typical normal concentration of UA in human urine blood are in micromolar (mM) range (~2 mM) and micro-molar (μM) range (120–450 μM) range, respectivly [1, 4]. Tryptophan (Trp) is well known as essential amino acid in human and herbivores bodies. [5]. However, it is present in greenery products and also it is added as a food fortifier to food products and medicinal [6]. In the real biological samples such as blood and urine, these compounds are co-existing. For example, AA coexists with DA and also UA in mammalian brain. In other hand, they are electroactive compounds with the same and/or nearly potential and the oxidation peaks of them overlapped in cyclic and differential voltammetry studies. So, it is almost impossible to detect them in one run by routine electroanalytical techniques. Therefore, the improvement of a selective method for simultaneous determination of AA, DA, UA and Trp is very attractive for analytical application and diagnostic research [7]. Several researches have been made for the simultaneous measurement of two or three of these compounds, but the quartnay determination of them has been considered less [6, 8-10].

Ammoniated ruthenium oxychloride, $[Ru_3O_2N_{14}H42]Cl_6$, (ARO) is an inorganic and polycationic dye (see Fig. 1).

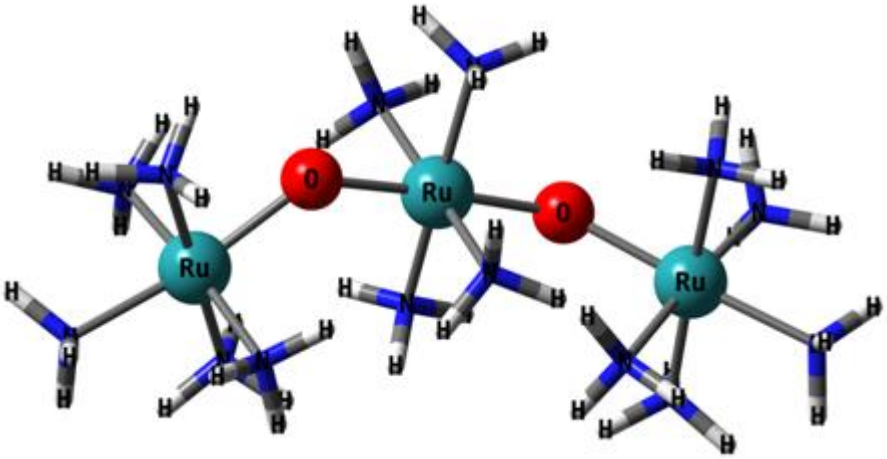

Figure 1. The chemical structure ARO.

It is used as a pharmacological tool for specific cellular mechanism studies and also in histology to stain aldehyde fixed mucopolysaccharides. Selectivity is an important issue in such studies as It is know that ARO interact with proteins [11]. Indeed, ARO displays as a potent inhibitor for intracellular calcium release by Ryanodine receptors [12]. Teixeira et al has been supported ARO on Y-type zeolite for detection of L-dopa [13].

To the best of our knowledge, no ARO has been reported to the simultaneous determination of AA, DA, UA, and Trp. We reported previously that modified GCE by iron ion-doped natrolite zeolite-multiwall carbon nanotube has good performance for simultaneous determination of AA, DA, UA, and Trp [10]. In this paper, a modified GC electrode is introduced for simultaneous determination of AA, DA, UA, and Trp in human serum and urine samples and proposes the advantages of high sensitivity,

low cost, and simple and fast construction. This modified GC electrode is based on immobilization of ARO on the functionalized multi-walled carbon nanotubes ($MWCNT_f$) dispersed in Nafion (NF). The modified electrode oxidized AA, DA, UA and Trp in phosphate buffer solutions (PBS) with pH = 4 to four well-defined peaks in cyclic voltammometry (CV) and linear sweeping voltammometry (LSV) techniques.

2. EXPERIMENTAL

2.1. Reagents and materials

AA, DA, UA and Trp, ARO and Nafion (5%) (NF) were purchased from Sigma–Aldrich and Merck Companies and used as received. The stock solutions of AA (0.01 M), DA (0.01 M) and Trp (0.001 M) were daily prepared by dissolving ascorbic acid, dopamine hydrochloride and Tryptophan in doubly distilled water (DDW). The stock solution of UA solution (0.01 M) was prepared by dissolving the solid in a small volume of 0.1 mol L^{-1} NaOH solution then diluted to reach final concentration. The solution was covered with aluminum foil and stored in a refrigerator. Multi-walled carbon nanotubes with nanotube diameters, OD = 20-30 nm, wall thickness = 1 - 2 nm, length = 0.5 - 2 μm and purity of > 95% was purchased from Aldrich. A series of phosphate buffer solutions (PBS) including H_3PO_4 were prepared and pHs were adjusted with NaOH (0.1 M) in the range from 2.0 to 8.0. Acetic acid (pK_a = 4.75) was used to prepare buffer solution with pH 4.0, 0.1 mol L^{-1} NaOH was used to to adjust pH to desire pH values. The electrolyte solutions were bubbled with pure nitrogen gas (99.999%) before each experiment.

2.2. Apparatus

Transmission electron microscopy (TEM) images were achieved with a Philips CM120 transmission electron microscopy with 2.5 ˚A resolution. FTIR spectra was performed in transmission mode using Valor III (JASCO) with a MCT detector. The energy resolution was adjusted to 1 cm^{-1}. All electrochemical measurements were carried out with an SAMA500 Electroanalyser (SAMA Research Center, Iran) equipped by a personal computer. A modified GCE as a working electrode, a saturated calomel electrode (SCE) as reference electrode and a platinum electrode were used in the three-electrode cell.

2.3. Preparation of the working electrode

Functionalized $MWCNT_f$ purification was performed by vigorously stirring in a mixture of sulfuric acid and nitric acid with the ratio of 3:1 at 25˚C for 24 h. This pretreatment eliminates impurities and generates adequate functional groups on the surface of $MWCNT_f$ [14]. The purified $MWCNT_f$ were filtered by centrifugation (2,000 rpm) and rinse with DDW until the pH of the filtrate

increased to 7.0. After more washing and drying, 25 mg of $MWCNT_f$ was sonicated in 1.0 mL of ARO solution (0.004 M) and 50µL NF for 2 h. The modifier was denoted as ARO-$MWCNT_f$-NF.

The GCE with 3mm diameter was polished with 0.05 µm alumina slurry on polishing cloth with water and then thoroughly rinsed with distilled water and finally sonicated in a mixture of water ethanol (9:1 v/v) for 3 min. The GCE was cycled in deoxygenated 1.0 M sulfuric acid using cyclic voltammetry between until a stable cyclic voltammetric profile (≈ 15 times) was reached. The clean GCE was coated by dropping 5.0 µL of the ARO-MWCNTf-NF suspension and then electrode was dried under infrared radiation for fast drying. This modified GC electrode was denoted as GC/ARO-$MWCNT_f$-NF. When electrode was not in use, it was stored in doubly distilled water. The GC/$MWCNT_f$-NF and GC/ARO-NF were also prepared with the same method.

3. RESULTS AND DISCUSSION

3.1. FTIR, TEM and electrochemical characterization of ARO-$MWCNT_f$

The FTIR spectra of ARO, functionalized $MWCNT_f$, immobilized ARO on functionalized $MWCNT_f$ and TEM of ARO-$MWCNT_f$ are shown in Figure 2.

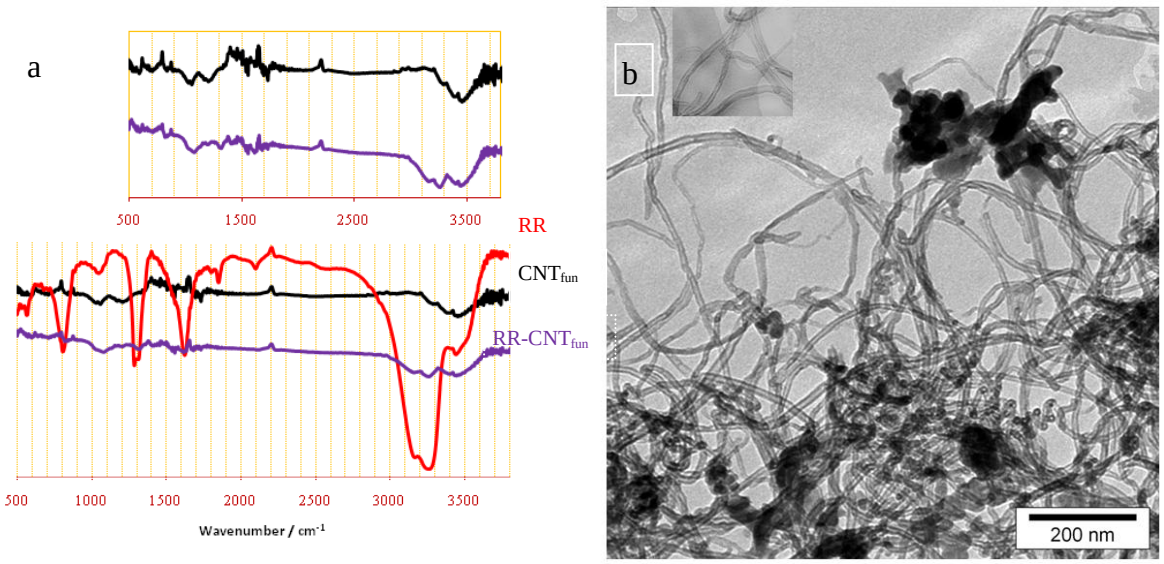

Figure 2. (a) FTIR spectra of the ARO, $MWCNT_f$ and immobilized ARO on functionalized $MWCNT_f$ and (b) TEM image of ARO-$MWCNT_f$-NF (Inset, $MWCNT_f$-NF)

Based on Fig.2a, the pure ARO shows several stronger peaks at 800, 1290, 1347, 1630 and broad peaks between 3100 and 3300 cm^{-1}. The functionalized $MWCNT_f$ shows new peaks at 670, 1050, 1130, 1545, and broad peaks between 3150-3550 in comparison with the FT-IR spectrum of the untreated MWCNTf (It is not shown), which lack the hydroxyl and carbonyl groups. With comparison of FTIR spectra of the ARO and functionalized MWCNTf with immobilized ARO on functionalized $MWCNT_f$, the peaks

around 800, 1290, 1347, 1630 cm^{-1} and broad peaks between 3100 and 3300 cm^{-1} have been assigned for immobilize ARO on functionalized $MWCNT_f$.

TEM images of pure functionalized $MWCNT_f$ and immobilized ARO on functionalized $MWCNT_f$ in NF are shown in Figure 2b. In the presence of NF, the $MWCNT_f$ and ARO-$MWCNT_f$ are not aggregate. Probably it is as a result of that NF can interact with $MWCNT_f$ and make huge entangled $MWCNT_f$ bundles from finer bundles.

Cyclic voltammograms of GC/ARO-$MWCNT_f$-NF in PBS in the selected Potential window at various scan rates from 10-1000 mV s^{-1} was examined (See Fig. 3a). Two redox pairs (oxidation and reduction peaks) at -0.187 and -0.291 V for the first and 0.484 and 0.939 for the second redox pair with potential peak separation (ΔE_p) 0.104 and 0.455 V were obtained, respectively. The peak currents for both oxidation and reduction peaks increased, with increase in scan rates. The anodic and cathodic peak currents are linearly proportional of the scan rates. The corresponding plots for the anodic peak current (I_{pa}) and catodic peak current (I_{pc}) as a function of scan rate (υ) have been demonstrated in Figs. 3b and c for the first and second redox pairs, respectively. Plots of the peak currents *versus* the scan rate for both redox pairs (Fig. 3b and c) are linear in two sweep rate stages of 10–150 and 150-1000 mVs^{-1}, proving a surface-controlled electrode processes [4, 10]. Furthermore, the anodic peak potential is shifted positively and cathodic peak potential shifted negatively with increasing of the scan rate and both the peak potentials are linearly dependent on ln(*v*). For both couples, the ratios of the anodic-to-cathodic peak currents are close unity.

These behaviors are consistent with a diffusionless system [15] and the redox reactions to be quasi-reversible electron transfers. The both couples peaks can be regarded to redox reactions of ARO ($[Ru^{III}–Ru^{IV}–Ru^{III}]$) encapsulated in NF to ARO-brown (ARO_b) ($[Ru^{IV}–Ru^{III}–Ru^{IV}]$) [12] and then ARO_b to ($[Ru^{V}–Ru^{II}–Ru^{V}]$, assumed to be a one-electron transfer:

$$[(NH_3)_5Ru^{III}–O–Ru^{IV}(NH_3)_4–O–Ru^{III}(NH_3)_5]^{6+} \rightarrow [(NH_3)_5Ru^{IV}–O–Ru^{III}(NH_3)_4–O–Ru^{IV}(NH_3)_5]^{7+} + e- \quad (1)$$

$$[(NH_3)_5Ru^{IV}–O–Ru^{III}(NH_3)_4–O–Ru^{IV}(NH_3)_5]^{7+} \rightarrow [(NH_3)_5Ru^{V}–O–Ru^{II}(NH_3)_4–O–Ru^{V}(NH_3)_5]^{8+} + e- \quad (2)$$

Based on Sharp *et al.* method [16], the surface coverage of the modified GC/$MWCNT_f$–ARO-NF electrode can be estimated from slope Fig. 3b. According to this method, the peak high ($I_p = (n^2F^2A\Gamma v)/(4RT)$ is relevant to the surface concentration of electroactive species, Γ. In this equation, *n* is number of electrons in such a reaction equation, A is the geometric surface area of the electrode with radius, r = 1 mm, (0.0314 cm^2), Γ (mol cm^{-2}) is the surface coverage, $v\ (mV\ s^{-1})$ is the scan rate, and R is gas constant = 8.314 J/mol.K, *F* is Faraday's constant, (96485 C/mol) and *T* is temperature (K). From the slope 0.214 of anodic peak currents *vs.* scan rate (Fig. 3b) the computed surface concentration of ARO in ARO-$MWCNT_f$-NF is 7.2×10^{-9} mol $cm^{-2}$for n = 1.

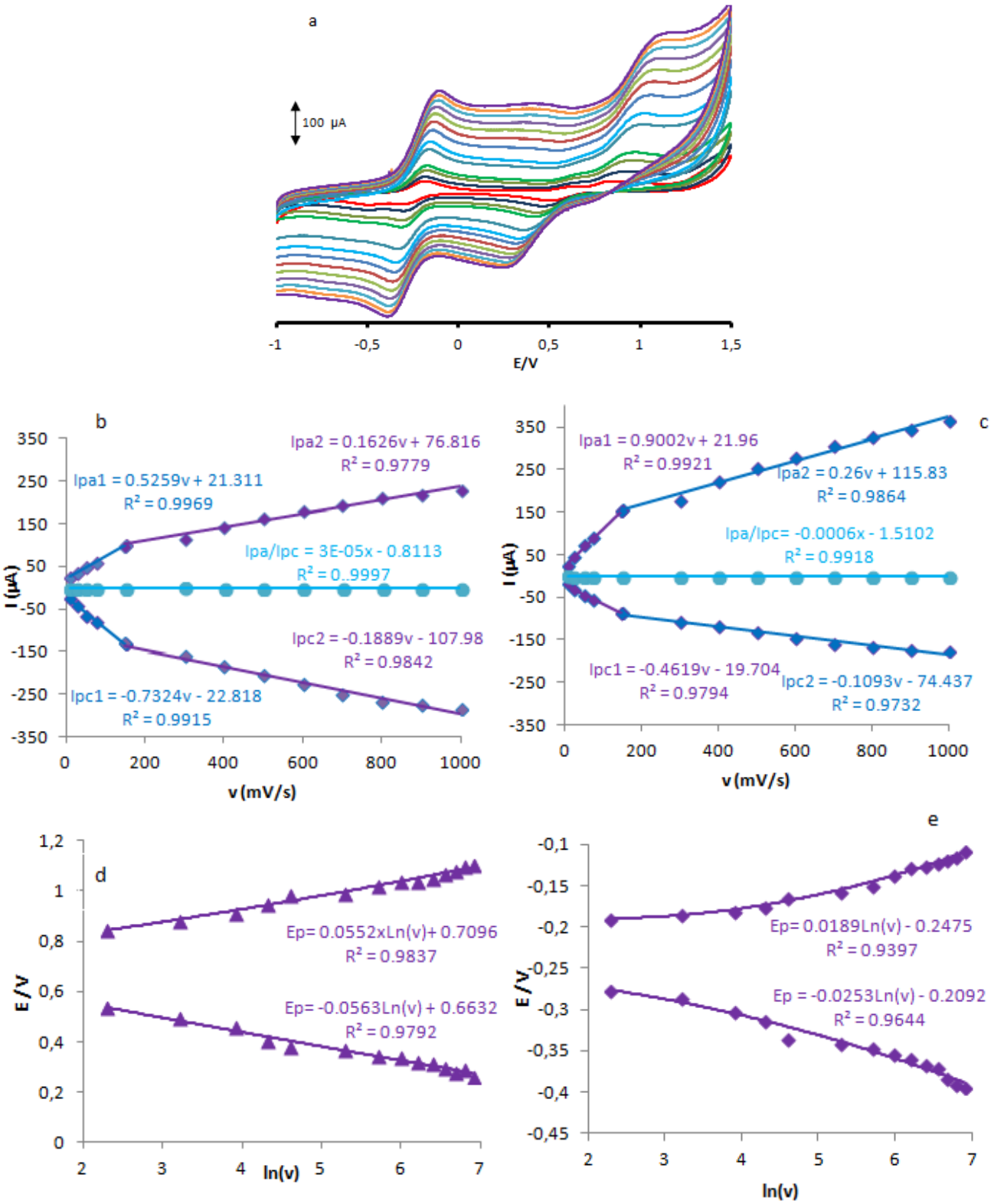

Figure 3. (a) CVs of GC/MWCNT$_f$–ARO-NF electrode in PBS (pH 4) at various scan rates (from inner to outer curve): 10, 25, 50, 75, 100, 150, 300, 400, 600, 700, 800, 900 and 1000 mV s^{-1} and (b) the plot of peak currents *vs.* scan rates (for first redox peak), (c) the plot of peak currents *vs.* scan rates (for second redox peak), d) the plot of peak potential *vs.* scan rates (for first redox peak) and e) the plot of peak potential *vs.* scan rates (for second redox peak).

3.2. Compression studies of different modified electrodes for simultaneous determination

Cyclic voltammograms (CVs) of a mixture solution of AA, DA, UA and Trp at bare GCE (BGCE) and different modified electrode such as GC/ARO-NF, GC/MWCNTf-NF and GC/ARO-MWCNT$_f$-NF have been shown in Fig. 4.

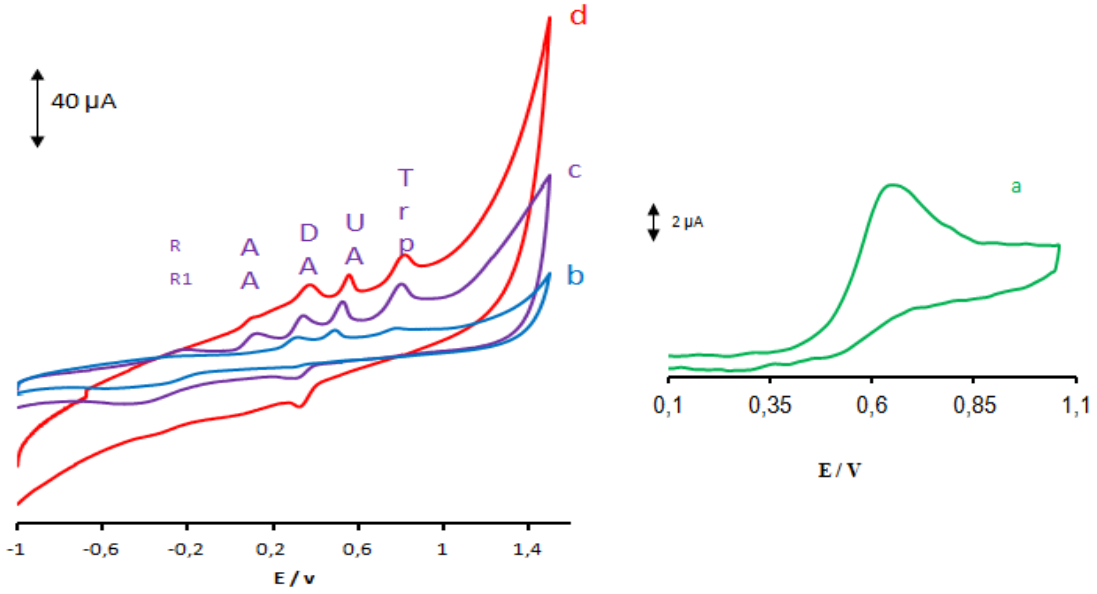

Figure 4. CVs at (a) BGCE (b) GC/ARO-NF, (c) GC/ARO-MWCNT$_f$-NF, (d) GC/MWCNT$_f$-NF electrodes in the presence of AA, DA ,UA and Trp in PBS (0.1 M) at pH 4.0. Scan rate: 100 mV s^{-1}.

Based on the Fig.4a, BGCE did not showed oxidation peaks for AA, DA, UA and Trp. It is not possible to distinguish the oxidation potential of AA, DA, UA and Trp in the BGCE. Based on this result, the BGCE is not adequate for the simultanous detection of a mixture of AA, DA, UA and Trp. Figs. 4b-d shows the CVs of a quaternary mixture at GC/ARO-NF, GC/MWCNT$_f$-NF, GC/ARO-MWCNT$_f$-NF modified electrodes. Two later modified electrodes oxidized AA, DA, UA and Trp in four well-separated CV peaks with improved oxidation current response increase as follows: GC/MWCNT$_f$-NF> GC/ARO-MWCNT$_f$-NF (see Fig. 4c, d) and GC/ARO-NF did not shown any oxidation peaks for AA (see Fig. 4b). The results were summarized in Table 1. As it can be seen in Fig. 4c, the GC/MWCNT$_f$-NF showed a higher enhancement in the oxidation peak current of DA, UA and Trp but a slight growth of the oxidation peak current of AA compared with GC/ARO-MWCNT$_f$-NF. Based on our previous work for simultaneous measurement of a ternary mixture of AA, DA and UA using a modified GC electrode with only MWCNT, the peak current of AA and also two others compounds DA and UA raised with increasing of AA concentration when DA and UA were kept in a constant concentration [17]. Similarly and obviously, keeping the concentrations of other two compounds constant, the oxidation peak current of AA or UA/DA were increased too. This proved that the modified GC electrode with only MWCNT is not appropriate for the stable simultaneous determination of the biocompounds. In the other hands, the GC/ARO-MWCNT$_f$-NF indicated an increase of the oxidation peaks current with adequate peak separations of AA, DA, UA and Trp. The proposed electrode oxidized AA, DA, UA and Trp at 0.09, 0.323, 0.511 and 0.782 V in four well-

defined CV peaks. As a result, application of the GC/MWCNT$_f$–ARO-NF results to the improvement of peak separation and current sensitivity and selectivity in detection of AA, DA, UA and Trp simultaneously. Moreover, the oxidation peaks of AA, DA, UA and Trp were more stable at the GC/ARO-MWCNT$_f$-NF modified electrode in the subsequent cycles. The separations of oxidation peak potentials of AA–DA, DA–UA and UA–Trp were of 233, 188 and 271 mV, respectively which were enough for the measurement of this quaternary mixture in the meantime.

Table 1. Comparison of E_{pa} at the surface of different electrodes in PBS (pH 4.0) containing 4.0×10^{-5} mol L^{-1} AA, DA, UA and Trp. Scan rate, 100 mVs^{-1}.

Modified electrode Type	Analytes			
	AA	DA	UA	Trp
GC/ARO-NF	-	0.276	0.458	0.742
GC/MWCNT$_f$-NF	0.075	0.342	0.545	0.791
GC/ARO-MWCNT$_f$-NF	0.09	0.323	0.511	0.782

3.3. Scan rate and pH effects

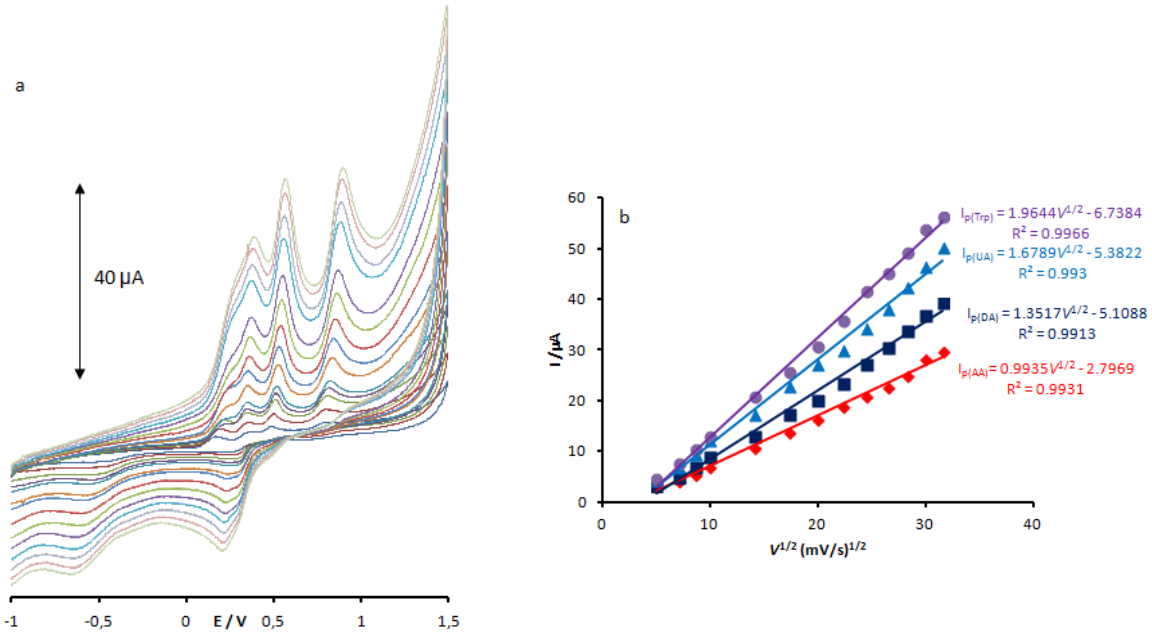

Figure 5. CVs of GC/MWCNT–ARO-NF in PBS (pH 4.0) in the presence of AA, DA, UA and Trp at various scan rates (from inner to outer curve) 10, 25, 50, 100, 150, 300, 400, 500, 600, 700, 800, 900 and 1000 mVs^{-1}, (b) Plot of peak currents *vs.* $v^{1/2}$ for AA, DA, UA and Trp.

Fig. 5 was shown the CVs of AA, DA, UA and Trp at GC/ARO-MWCNTF-NF at various scan rates in the PBS at pH 4.0 which can be suggested that, its kinetics are controlled by mass transport of spices from bulk to the electrode surface, as there is a linear correlation between the I_{pc} and $v^{1/2}$; however, at higher scan rates, peak separation of AA and DA was not satisfactory for analysis and some deviations from linearity were also observed. It is clear that the anodic oxidation peak potential (E_p), for AA, DA, UA and Trp shifts softly while scan rate increases to higher rates. These results show that a kinetic limitation exists while GC/ARO-MWCNT$_f$-NF composite is reacting with AA, DA, UA and Trp. Finally, concerning our investigation to reach best efficiency for peak separation and peak currents, 100 mV s^{-1} was chosen as optimal scan rate.

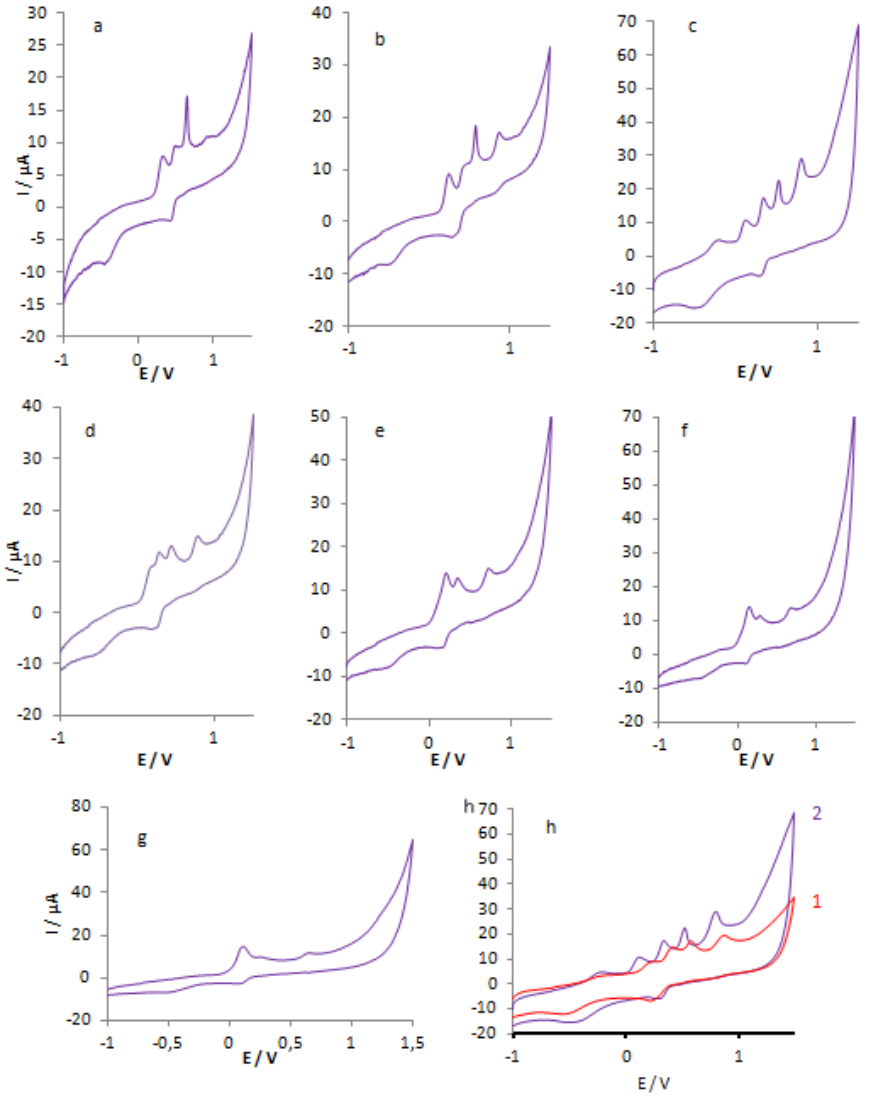

Figure 6. CVs of GC/MWCNT$_f$–ARO-NF in the presence of AA, DA, UA and Trp at various pH (a) 2, (b) 3, (c) 4, (d) 5, (e) 6, (f) 7, (g) 8 on the peak separation and peak current for the oxidation of AA, DA, UA and Trp; pH= 2.0, 3.0, 4.0, 5.0, 6.0, 7.0 and 8.0 (PBS 0.1M). (h) Comparison of CVs of GC/MWCNT$_f$–ARO-NF in the presence of AA, DA, UA and Trp at acetate buffered solution(curve 1) and phosphate buffered solution (curve 2) (0.1 M) at pH 4.0. Scan rate: 100 mV s^{-1}.

The oxidation of AA, DA UA and Trp is pH dependent. Hence, the electrochemical response of the GC/ARO-MWCNT$_f$-NF towards the oxidation of AA, DA UA and Trp in different pHs has been studied. A series of PBS (0.1 mol L^{-1}) and acetate buffer (0.1 mol L^{-1}) solutions were prepared and tested as supporting electrolyte. The peak separation and peak current in various pH range from 2.0 to 8.0 are shown in Fig. 6a-g.

According to the results, the anodic peak currents of AA, UA and Trp grow with increasing of the solution pH from 1.0 to 4.0 and decreases while pH increases to 6.0. But the anodic peak current of DA increase with rising pH until it reaches to 5.0 and then its peak current decreases by increasing pH to 6.0. There is a slight change in anodic peak current of AA, UA, DA and Trp with rising pH from 6 to 8.0. It must be considered, there is an overlap in the anodic peak potentials of AA and DA in pH higher than 5.

Finally, Fig. 6h indicates two different buffered electrolyte which were tested in same conditions for acetic acid buffer solution (AABS) and PBS (0.1 mol L^{-1} with pH 4.0). Based on Fig. 6h, the highest peaks separation and satisfactory peak currents and negatively shifts for PBS (Fig. 6h$_1$) are better than AABS (Fig 6h$_2$). The effect of pH variation on the anodic peak currents of AA, DA UA and Trp was shown in Fig. 7a. Moreover, the anodic peak potentials of AA, DA UA and Trp were declined linearly when pH increased from 1.0 to 8.0, which indicates proton involvement in electrode processes (see fig. 7b).

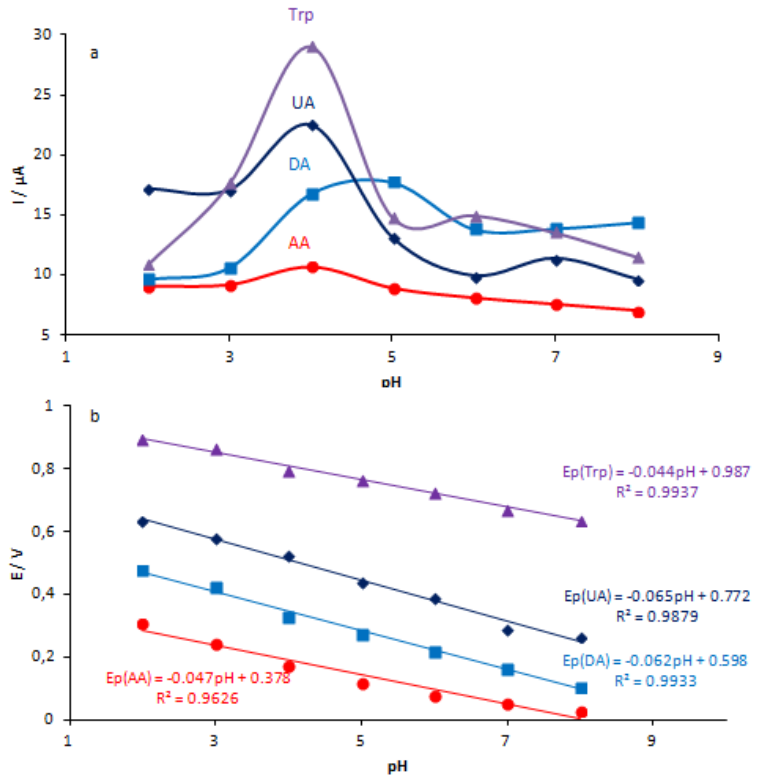

Figure 7. (a) Plot of peak currents *vs.* pH and (b) plot of peak potential *vs.* pH for the oxidation of AA, DA, UA and Trp for CVs of Fig. 6.

It was detected that the anodic peak potentials for UA, AA and DA shifted to negative potentials while pH is increasing which was regarded because of the participation of proton(s) in the

oxidation reactions of AA, DA, UA and Trp. for example, the oxidation reaction of DA can be described for DA as follow:

$$DA_{Red} - mH^+ - ne \longleftrightarrow DA_{Ox} \quad (3)$$

where m and n are the number of protons and electrons participating the reaction. The anodic peak potentials for peak Red, is given by [18]:

$$E'_{DA(Red)} = E_{DA(Red,\ pH=0)} - (2.303\ mRT/(nF))pH \quad (4)$$

where $E_{DA(Red,\ pH=0)}$ is the anodic peak potential for Red at pH= 0.0, and R, T, and F have their usual meanings. The values of $E_{DA(Red)}$ is plotted in Fig. 7b. As can be seen in Fig. 7b, $E'_{DA(Red)}$ was moved to negative potentials with the slope of 0.062V/pH, which is in agreement with the theoretical slope (-(2.303 mRT/(nF)) of 0.059(m/n) V/pH. This result reveals that oxidation of DA involves an equal number of protons (m) and electrons (n) (m=n) [19, 20]. Also, the slope for AA, UA and Trp are 0.047, 0.065 and 0.44 V/pH. Based on these results, the oxidation of AA, DA UA and Trp at the surface of GC/ARO-MWCNT$_f$-NF were explained in Eqs. 5-8.

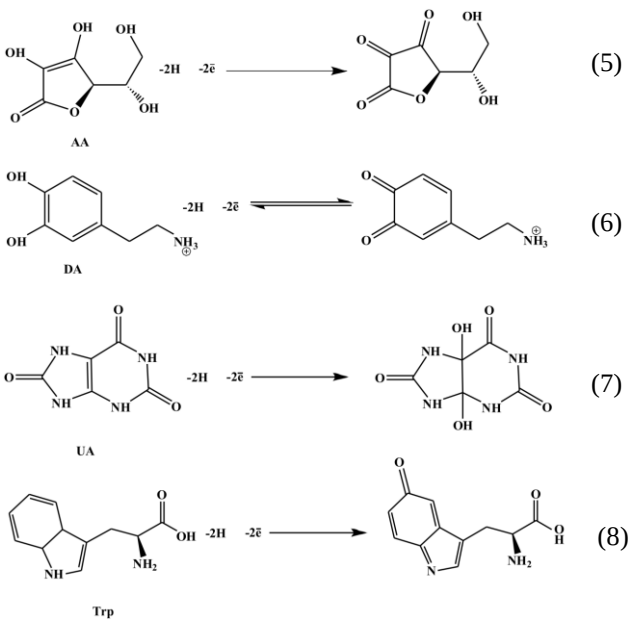

(5)

(6)

(7)

(8)

A phosphate buffer with pH 4.0 was selected as optimal pH which referred to satisfactory peak potential separation and highest anodic peak current for simultaneous determination of AA, DA UA and Trp.

3.4. Interference studies

One of the main drawbacks of simultaneous determination of AA, DA, UA and Trp in presence of other electrochemically active compounds are interferences caused by these biocompounds in real samples, which can be oxidized under same potentials. As oxidation peak potential of AA, DA, UA and Trp is close to each other and they usually coexist in biological samples interference from these compounds are important [10, 19]. Hence, the mixed solution technique [10, 21] was applied to study

the effect of interferences on electrochemical detection of AA, DA, UA and Trp. The electro-oxidation processes of AA, DA, UA and Trp at GC/MWCNT-RR-NF in the solution have also been carried out when the concentration of one species increased, while other 3 species are kept constant and the results are reported in Fig. 8. Evaluation of Fig. 8a reveals that the peak current of AA grows by increasing of AA concentration in a mixture with constant concentration of DA, UA and Trp.

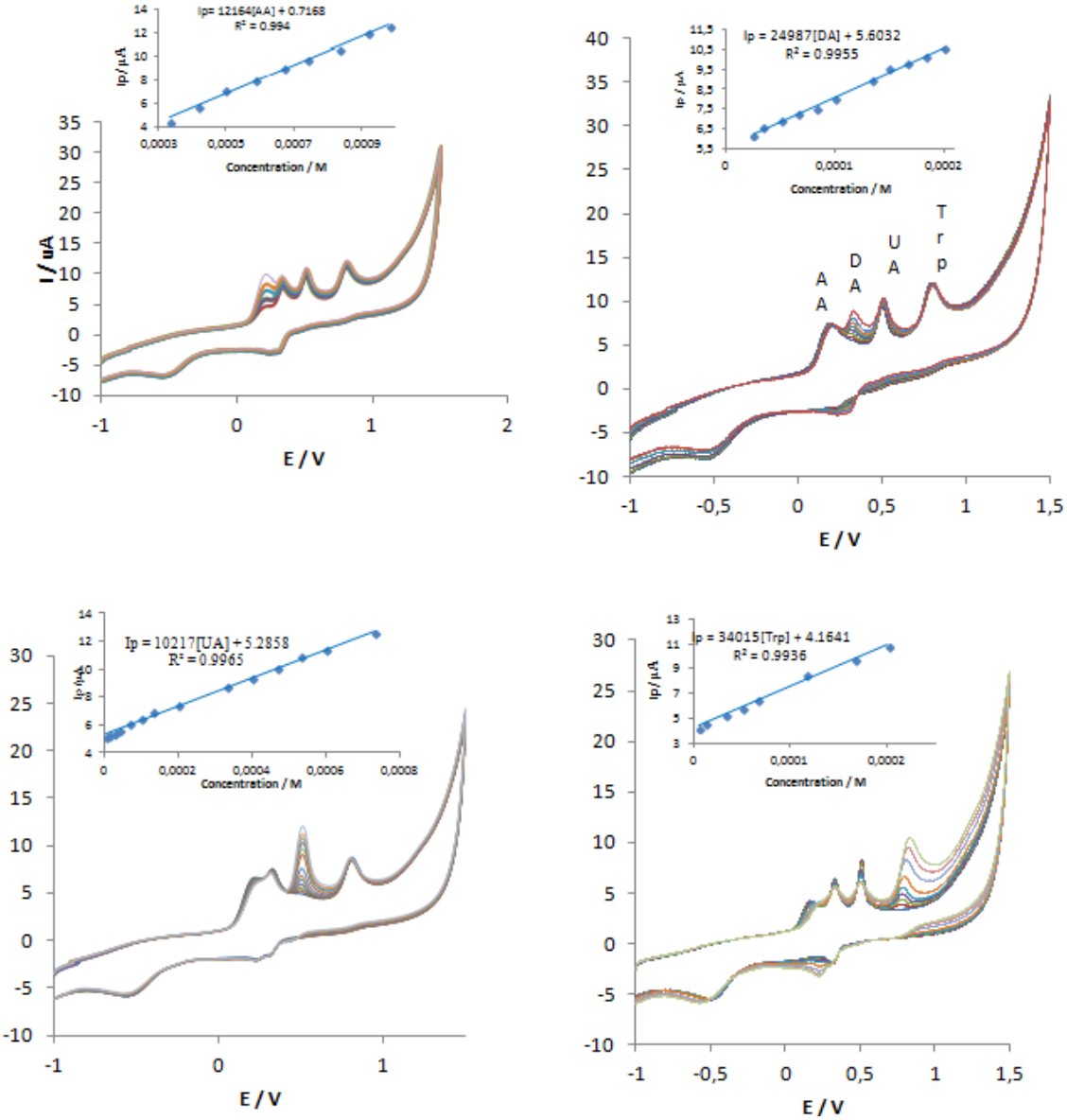

Figure 8. CVs at the GC/ARO-MWCNT$_f$-NF electrode in 0.1 M PBS with pH 4.0 (a) containing DA (100.0 µM) UA (133.3 µM), (Trp (50.5 µM) and different concentrations of AA (from inner to outer):333.3, 413.1, 495.2, 583.5, 667.1, 583.1, 739.2 µM, (b) Containing AA (583.5 µM) UA (133.3µM), (Trp (50.5 µM) and different concentrations of DA (from inner to outer): 25.0, 33.3, 50.0, 83.3, 100.0, 133.3, 150.0, 166.7 µM, (c) Containing AA (583.5 µM) DA (100.0µM), Trp (50.5 µM) and different concentrations of UA (from inner to outer):6.6, 13.3, 26.6, 40.0, 66.6, 100.0, 133.3, 200.0, 333.3, 400.0, 466.7, 533.3, 600.0, 733.3 µM and (d) Containing AA (583.5µM) DA (100.0 µM), UA (133.3 µM) and different concentrations of Trp (from inner to outer): 6.6, 13.3, 33.3, 50.0, 66.6, 116.6, 166.7, 200.0 µM,

The charge current was increased after AA was oxidized, but the peak currents of DA, UA and Trp did not change. Similarly, as shown in Fig. 8b, c and d, when keeping the concentrations of the other 3 compounds constant, the oxidation peak currents of DA or UA or Trp were proportional to their concentration, while other 3 compounds did not change. The others biological compounds, such as Try, Glu up to 1200 μM and Cys up to 900 μM did not significantly interfered with the measurement of AA, DA and UA (250 μM). Also, no serious interference for the detection of AA, DA, UA and Trp (200 μM each) was seen from the following compounds: NaCl and KCl (3500 μM), $CaCl_2$ and $ZnCl_2$ (4000 μM) and $MgSO_4$ (3500 μM). The above results illustrate that the proposed modified electrode is selective and sensitive for the simultaneous measuring of AA, DA, UA and Trp in presence of other compounds which exists in real sample.

3.5. Calibration curve

According our experimental results reported above, it can be seen that in the quaternary mixture containing AA, DA, UA and Trp when a GC/MWCNT$_f$–ARO-NF was employed, the oxidation peaks of these 4 compounds were obviously separated from each other, but they were not well separated when the other modified electrodes were used. If the concentrations of AA, DA, UA and Trp increased synchronously, on increasing the concentrations of the 4 compounds, the peak currents at the GC/MWCNT$_f$–ARO-NF electrode increase accordingly as shown in Fig. 9. The calibrations were linear in the range of 2.33–176.8 μM, 1.30–300 μM, 1.05–310 μM and 1.33–326 μM, for AA, DA, UA and Trp, respectively. The detection limits were achieved using the equation $Y_{LOD} = X_B + 3S_B$, where Y_{LOD} is the signal for detection limit, X_B the mean of blank signal and S_B the standard deviation of the blank signal [22]. The theoretical detection limits of the proposed sensor for AA, DA, UA and Trp were 1.5, 0.64, 0.57 and 0.61 μM, respectively.

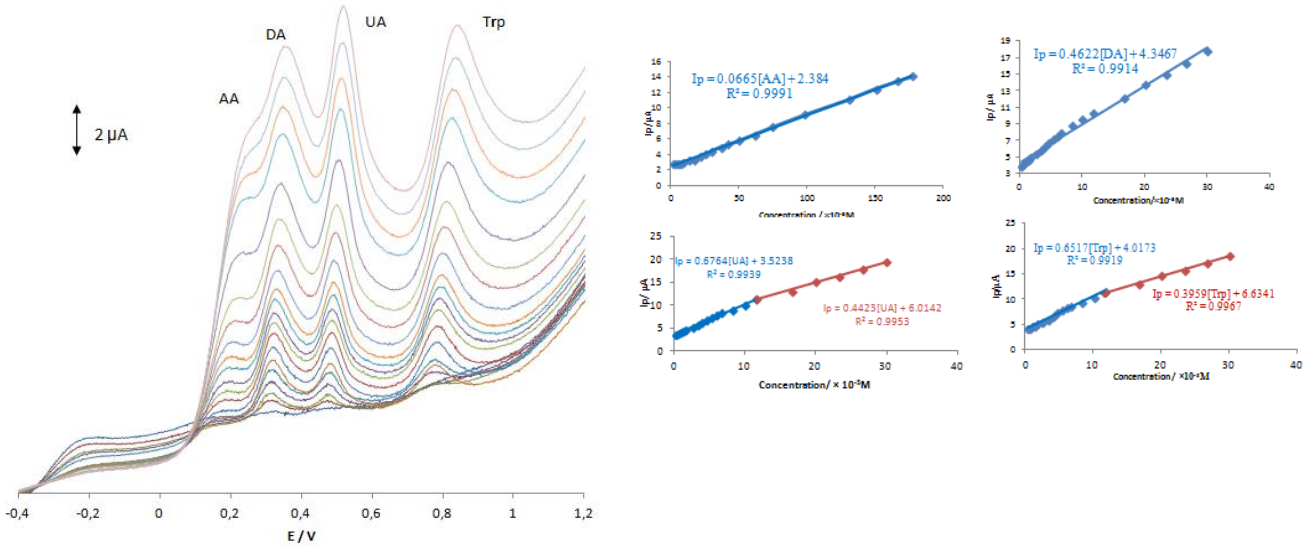

Figure 9. LSVs of the mixture containing AA, DA, UA and Trp at the GC/MWCNT$_f$–ARO-NF electrode in PBS (pH 4.0) at the scan rate of 100 mV s^{-1}, (Inset, Calibration curves for analytes).

3.6. Real samples

The real samples such as Human serum and urine samples as real sample were selected for analysis using the standard addition method. In order to prevent interferences of matrix and to fit in linear range of AA, DA, UA and Trp, the experiment was carried out with only 2 ml of real samples which were added to the electrochemical cell containing 15 ml of phosphate buffer solution. The recovery of the spiked samples was between 95.1% and 104.4% (Table 2). In addition, RSD (%) of all species (n=3), were less than 3.0 % as shown in Table 2.

Table 2. Determination of AA, DA, UA and Trp in human serum and urine samples using GC/MWCNT$_f$–RR-NF (n = 3).

Sample	Analyte	Detected(μM)	Added(μM)	Found(μM)	Recovery(%)
Serum	AA	-	45.0	43.8	97.3
	DA	-	25.0	26.1	104.4
	UA	-	50.0	51.1	102.2
	Trp	-	25.0	24.4	97.6
Urine	AA	-	40.0	39.1	97.8
	DA	-	40.0	38.7	96.8
	UA	2.4	45.0	48.0	101.3
	Trp	1.1	25.0	24.8	95.1

4. CONCLUSIONS

A new modified GCE with MWCNT$_f$–ARO -NF has been used for simultaneous determination of AA, DA, UA and Trp. The modified sensor not only increases and improves anodic peak current toward the oxidation of analytes, in addition resolves the overlapped oxidation peaks of AA, DA, UA and Trp at potentials 0.09, 0.323, 0.511 and 0.785 V, respectively. These results clearly revealed that ARO-MWCNT$_f$ is able to be used as an efficient promoter to increase the kinetics of the electrochemical process of AA, DA, UA and Trp. Comparison between GC/MWCNT$_f$-NF, GC/ARO-NF and GC/ MWCNT$_f$–ARO -NF demonstrates that GC/MWCNT$_f$–ARO -NF improve the simultaneous detection of AA, DA, UA and Trp with desirable stability, sensitivity and selectivity. In Table 3, this work has been compared with other reported works on modified electrodes in figures of merit such as linear range, limit of detection. Based on the data in Table 3, the proposed sensor seems to present a useful alternative for the simultaneous determination of AA, DA, UA and Trp in real samples with desirable results. A simple fabrication procedure, a wide linear range, enough stability and high reproducibility, propose this electrode as a good, cheap and a favorable candidate for practical applications.

Table 3. Comparison the proposed method with other electroanalytical methods with GC/MWCNTf-RR-NF electrodes for the simultaneous determination of AA, DA, UA and Trp.

Electrode	Modifier	pH and Buffer	Method	Analyte	Linear range (μM)	Detection limit (μM)	Ref
GC	Hemin-graphene oxide-pristine carbon nanotubes complexes	6 PBS	DPV	AA	0.5 to 2160	0.17	8
				DA	0.05–2.65 ,	0.017	
				UA	0.05 to 1.49	0.017	
				Trp	0.05–2.65	0.017	
GC	silver nanoparticles -decorated reduced graphene oxide	3.5, PBS	LSV	AA	10 - 1000	-	9
				DA	10 - 1000	-	
				UA	10 - 1000	-	
				Trp	10 - 1000	-	
GC	Fe-mesoporous polyaniline	3.5, PBS	CV	AA	10-300	6.5	10
				DA	10-300	9.8	
				UA	10-300	5.3	
				Trp	10-300	5.2	
GC	iron ion-doped natrolite zeolite-multiwall carbon nanotube	1.0, DCAAB	CV	AA	7.77–833	1.11	11
				DA	7.35–833	1.05	
				UA	0.23–83.3	0.033	
				Trp	0.074–34.5	0.011	
GC	ARO-MWCNTf-NF	4.0, PBS	LSV	AA	2.33–176.8	1.5	-
				DA	1.30–300	0.64	
				UA	1.05–310	0.57	
				Trp	1.33–326	0.61	

ACKNOWLEDGEMENT
The authors wish to thank from USB research council for financial support of this work.

References

1. S. Lupu, A. Mucci, L. Pigani, R. Seeber, C. Zanardi, *Electroanalysis*, 14 (2002) 519-525.
2. P. Ramesh, S. Sampath, *Electroanalysis*, 16 (2004) 866-869.
3. C.R. Raj, T. Okajima, T. Ohsaka, *J. Electroanal. Chem*., 543 (2003) 127-133.
4. M. Noroozifar, M. Khorasani-Motlagh, *Talanta*, 61 (2003) 173-179.
5. Y. Zhang, Z. Xia, H. Liu, M. Yang, L. Lin, Q. Li, *Sens. Actuators B Chem*., 188 (2013) 496-501.
6. G. Chen, J. Cheng, J. Ye, Fresenius' *J. Anal. Chem*., 370 (2001) 930-934.
7. V.S. Ijeri, P.V. Jaiswal, A.K. Srivastava, *Anal. Chim. Acta*, 439 (2001) 291-297.

8. B. Kaur, T. Pandiyan, B. Satpati, R. Srivastava, *Colloids and Surfaces B: Biointerfaces*, 111 (2013) 97-106.
9. M.A. Prathap, R. Srivastava, *Sens. Actuators B Chem*., 177 (2013) 239-250.
10. M. Noroozifar, M. Khorasani-Motlagh, R. Akbari, M.B. Parizi, *Biosens. Bioelectron*., 28 (2011) 56-63.
11. F. Vincent, M. AJ Duncton, *Curr. Top. Med. Chem*., 11 (2011) 2216-2226.
12. L.X.A. Tripathy, D.A. Pasek, G. Meissner, *Ann. N. Y. Acad. Sci*., 853 (1998) 130-148.
13. M.F. Teixeira, M.F. Bergamini, C.M. Marques, N. Bocchi, *Talanta*, 63 (2004) 1083-1088.
14. Y. Lin, X. Cui, X. Ye, *Electrochem. Comm*., 7 (2005) 267-274.
15. A.P. Brown, F.C. Anson, *Anal. Chem.*, 49 (1977) 1589-1595.
16. M. Sharp, M. Petersson, K. Edström, *J. Electroanal. Chem. Interfacial. Electrochem.*, 95 (1979) 123-130.
17. M. Noroozifar, M. Khorasani-Motlagh, A. Taheri, *Talanta*, 80 (2010) 1657-1664.
18. A. Afkhami, D. Nematollahi, L. Khalafi, M. Rafiee, *Int. J. Chem. Kinetics*, 37 (2005) 17-24.
19. H. Zhao, Y. Zhang, Z. Yuan, *Analyst*, 126 (2001) 358-360.
20. T. Imato, N. Ishibashi, *Biosens. Bioelectron*., 10 (1995) 435-441.
21. S. Mehretie, S. Admassie, T. Hunde, M. Tessema, T. Solomon, *Talanta*, 85 (2011) 1376-1382.
22. J.N. Miller, J.C. Miller, Statistics and chemometrics for analytical chemistry, Pearson Education, 2005.